Design of Supernumerary Robotic Limbs for the Augmentation of Astronauts Performing Partial-Gravity Extra-Vehicular Activities (EVAs)

Erik Ballesteros[1], Preston Rogers[2], Justin Jenkins[2], Kalind Carpenter[2], H. Harry Asada[1]
[1]Department of Mechanical Engineering, Massachusetts Institute of Technology, Cambridge, MA, USA
[2]Robotic Mobility and Manipulation Section, Jet Propulsion Laboratory, Pasadena, CA, USA
balleste@mit.edu

***Abstract*—This paper presents a design methodology for Supernumerary Robotic Limbs (SuperLimbs)—wearable robotic appendages intended to augment astronauts performing partial-gravity Extra-Vehicular Activities (EVAs) on the Moon. NASA has identified post-fall recovery as a high-risk process requiring an effective countermeasure. Human studies reveal that suited astronauts converge on a deterministic, sagittal-plane recovery path. A quasi-static biomechanical model quantifies the joint-torque gap between what a suited astronaut can exert and what the task demands. A two-phase design optimization-coarse-grid backtracking search over 5.4 million permutations followed by fine-grid localized parameter sweep-identifies a 4-degree-of-freedom SuperLimbs kinematic structure that minimizes actuator energy dissipation and CoM tracking error. The resulting Earth prototype, built at an anonymous research laboratory, successfully demonstrates a full prone-to-upright recovery and reduces the load borne by a human wearer by up to 55%. Critically, the deterministic recovery trajectories uncovered by this work provide a structured foundation for developing autonomous SuperLimbs control, enabling robots to act as intelligent safety partners for astronauts in future planetary missions.**

***Index Terms*—Supernumerary robotic limbs, wearable robotics, human augmentation, EVA, astronaut fall recovery, design optimization**

I. Introduction

NASA's Artemis Program aims to establish a sustained human presence on the Moon by the early 2030s [1]. Extra-Vehicular Activities (EVAs) are among the most hazardous mission elements: a pressurized Space Suit Assembly (SSA) introduces substantial mass penalties and severely restricts joint range of motion, shifting the body's center of mass (CoM) rearward [2]–[4]. Falling on the lunar surface has been a persistent risk since Apollo, and NASA has categorized post-fall recovery as a high-risk process requiring an effective countermeasure [5], [6]. Conventional solutions entail significant trade-offs in mobility, cost, or complexity [7], [8].

SuperLimbs offer a complementary path. Unlike exoskeletons, SuperLimbs adopt a kinematic structure independent of the wearer's posture, effectively providing the astronaut with an additional pair of appendages [9], [10]. In previous work, early SuperLimbs concepts and pilot studies for EVA were established [11], [12]. The present paper closes the loop from biomechanical requirement derivation through prototype validation, with the following contributions:

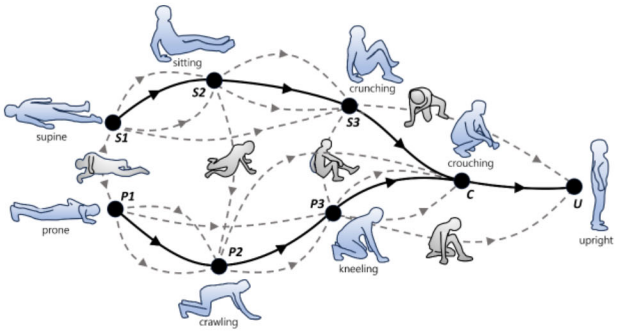

Fig. 1. Simple model representation of astronaut post-fall recovery.

1) A biomechanical model estimating astronaut joint torques and the gap that SuperLimbs must fill during post-fall recovery.
2) A two-phase optimization methodology that down-selects SuperLimbs kinematic designs from a 5.4-million-permutation space.
3) Fabrication and experimental validation of the Earth prototype.

II. Suited Post-Fall Recovery Analysis

A. Human Study Observations

Pilot studies using an analog space suit (mimicking the mass, inertia, size, and mobility of NASA's Extra-Vehicular Mobility Unit (xEMU)) revealed two key observations. First, recovery trajectories decompose into a sequence of statically stable *waypoints*: eg. Prone (P1→P2→P3), Crouching (C), and Upright (U). Second, while unsuited humans take diverse recovery paths, the space suit constrains all successful subjects to the same prone route: P1 $\rightarrow$ P2 $\rightarrow$ P3 $\rightarrow$ C $\rightarrow$ U. Motion is symmetric about the sagittal plane throughout, driven primarily by the rearward CoM shift imposed by the Portable Life Support System (PLSS).

B. Biomechanical Model

The suited astronaut is modeled as a 7-link quasi-static kinematic chain. The generalized coordinate vector is $\boldsymbol{X} = [\boldsymbol{x}_{\mathrm{CoM}}^T, \boldsymbol{\theta}_{\mathrm{body}}^T]^T$, where $\boldsymbol{x}_{\mathrm{CoM}}$ locates the system CoM and

$\boldsymbol{\theta}_{\text{body}} = [\phi_{\text{HUT}}, \theta_{sh}, \theta_{el}, \theta_{wr}, \theta_{hp}, \theta_{kn}, \theta_{ak}]^T$ captures posture. The Hard Upper Torso (HUT)-torso, chest, head, SSA, and PLSS is treated as a single rigid body whose CoM dominates the system.

At each recovery phase, a static bracing analysis gives the required joint torques:

$$\boldsymbol{\tau}_h = \boldsymbol{J}^T\big((m_h + m_{\text{ssa/plss}})\, g\big)\, \hat{z}, \tag{1}$$

where $\boldsymbol{J}^T$ is the Jacobian transpose and $\hat{z}$ is the vertical unit vector. When both limbs contact the ground, the load is shared by minimizing total squared torque [13]. The SSA joint stiffness torque $\boldsymbol{\tau}_{\text{ssa}}$ [14] is added to obtain the total required torque $\boldsymbol{\tau}_{\text{req},i} = \boldsymbol{\tau}_{h,i} + \boldsymbol{\tau}_{\text{ssa},i}$. Comparing $\boldsymbol{\tau}_{\text{req}}$ with the Anderson maximum voluntary joint torque model [15] reveals the *torque gap* that SuperLimbs must supply: $\boldsymbol{\tau}_{\text{gap}} = \max(\boldsymbol{\tau}_{\text{req}} - \boldsymbol{\tau}_{h_{\max}}, \mathbf{0})$. The most demanding phases are P1→P2 (hip and knee) and P3→C (ankle), where required torques substantially exceed voluntary capacity. The task-space SuperLimbs force is recovered via the pseudoinverse of the leg/arm Jacobians, yielding the required force trajectory shown in Fig. 2.

III. SuperLimbs Design Methodology

A. Parametric Model

A SuperLimbs design with m actuated joints is parameterized by an *intrinsic* matrix

$$\boldsymbol{D}^{3\times m} = \begin{bmatrix} \alpha_1 & \alpha_2 & \cdots & \alpha_m \\ l_1 & l_2 & \cdots & l_m \\ r_1 K_{m_1} & r_2 K_{m_2} & \cdots & r_m K_{m_m} \end{bmatrix}, \tag{2}$$

where α_i is the ith joint-axis angle, l_i the link length, r_i the gear ratio, and K_{m_i} the motor constant. Two *extrinsic* vectors complete the parameterization: the end-effector ground contact point $\boldsymbol{C} = [C_x, C_y, 0]^T$ and the base mounting location on the PLSS $\boldsymbol{d} = [d_x, d_y, d_z]^T$.

B. Functional Requirements

Candidate designs must satisfy four constraints: (1) **Reachability**—end-effectors must contact the ground throughout the CoM trajectory; (2) **Singularity avoidance**—configurations near kinematic singularities cause unstable joint motions and are excluded; (3) **No-slip contact**—ground contact forces must lie within the friction cone; (4) **Collision avoidance**—SuperLimbs links must not intersect the astronaut body volume.

C. Two-Phase Optimization

Phase 1 - Coarse-Grid Backtracking Search. Each parameter is discretized into 10 equally spaced values, yielding 5.4×10^6 design permutations. A backtracking algorithm [16] prunes branches that violate any functional requirement, reducing the viable set to **252 designs** for $m = 4$. These are ranked by (i) total actuator energy loss, (ii) end-effector tangential contact force (slip margin), and (iii) maximum link shear load.

TABLE I
CoM tracking error (3-link) vs. contact point offset from optimal $\boldsymbol{C}^*$

$\boldsymbol{C}$ [m]	L^∞ error	L^2 error
$[0.33, -0.30, 0]^T$	3.6×10^{-4}	6.2×10^{-4}
$[0.50, -0.30, 0]^T$	4.4×10^{-2}	4.6×10^{-2}
$[0.33, -0.50, 0]^T$	1.5×10^{-1}	2.5×10^{-1}
$[0.65, -0.65, 0]^T$	3.5×10^{-1}	1.8×10^{0}

Phase 2 - Fine-Grid Localized Optimization. The best Phase 1 design seeds a fine parameter sweep optimizing

$$\min_{\boldsymbol{D},\boldsymbol{C},\boldsymbol{d}} \int_0^{t_f} \boldsymbol{\tau}^T \boldsymbol{W} \boldsymbol{\tau}\, dt \;+\; \rho \sum_{i=1}^{N} \|\boldsymbol{x}_i - \boldsymbol{x}_{d,i}\|^2, \tag{3}$$

where $\boldsymbol{W} = \text{diag}(1/r_j^2 K_{m_j}^2)$ weights actuator energy dissipation and the second term penalizes CoM tracking error. The dynamics constraint $\boldsymbol{H}(\boldsymbol{\theta})\ddot{\boldsymbol{\theta}} + \boldsymbol{h} + \boldsymbol{g} + \boldsymbol{J}_{SL}^T \boldsymbol{F}_{SL} = \boldsymbol{\tau}$ is enforced throughout. Actuators are custom aerospace-grade units ($r = 160$, $K_m = 0.36$ Nm/$\sqrt{\text{W}}$, peak torque 400 Nm).

D. Optimal Design and Key Insights

The final design is a **4-DoF SuperLimbs** with all joint axes orthogonal ($\alpha_i = \pi/2$ rad), link lengths $[l_1, l_2, l_3, l_4] = [0.20, 0.61, 0.16, 0.69]$ m, and ground contact placed 0.37 m lateral and 0.18 m *rearward* of the astronaut CoM. Two insights emerge: (1) the structure mirrors human arm proportions, confirming computationally what biology has shaped through evolution; (2) rearward contact placement optimally expands the base of support where the PLSS-shifted CoM travels during P2→P3→C. By contrast, the 3-DOF design violates the no-slip constraint and incurs a ≈225 Nm singularity torque spike; the redundant 4th joint eliminates both pathologies while maintaining robust tracking across varied contact locations (see Table I for tracking error buildup of 3-DOF design).

IV. Prototype and Experimental Validation

A. Prototype Description

The physical prototype was fabricated at an anonymous research laboratory (Fig. 3). Each of the two arms contains four custom aerospace-grade actuators. Links are simple tube geometries except at joint 4, where a corner bracket realizes the required offset (l_1) and joint orientation while satisfying FEA-derived structural requirements (FOS = 2). The arms mount to an extruded aluminum backpack frame simulating a PLSS, powered via a 70 V off-board umbilical. Control is implemented in ROS2 over EtherCAT using a modified control framework [17], with each arm as an independent EtherCAT branch managed by a NUC onboard computer.

B. Experimental Results

Three metrics were evaluated using a 155 N nursing mannequin (approximating a 90 kg astronaut at lunar gravity, 146 N):

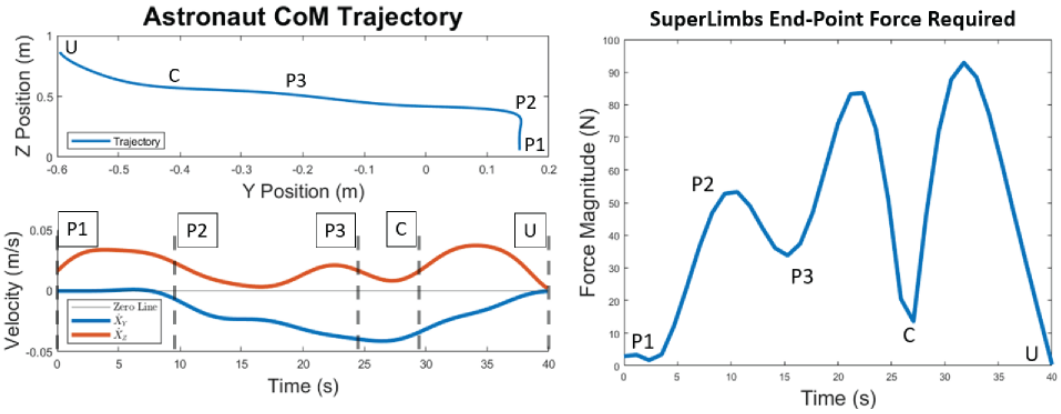

Fig. 2. Task-space CoM trajectory and required SuperLimbs reaction forces for post-fall recovery. Peak forces (≈90 N) occur during the P2 kneeling phase; forces approach zero during the quasi-static P2→P3→C cane-like bracing phases.

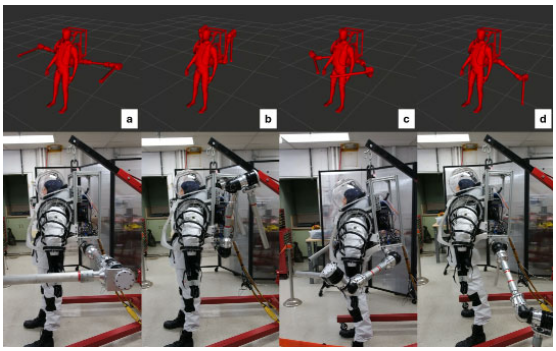

Fig. 3. The Earth prototype. A pair of 4-DoF arms mount to an aluminum PLSS-simulating backpack frame. Each arm is driven by four custom aerospace-grade actuators (peak torque 400 Nm).

TABLE II
KEY PERFORMANCE METRICS: MODEL VS. PROTOTYPE

Metric	Phase	Model	Prototype
Max Actuator Torque [Nm]	P1–P2	105	310
	P2–P3	12	74
	P3–C	15	95
	C–U	174	145
Max Power [W]	P1–P2	4	32
	P2–P3	1	3
	P3–C	1	4
	C–U	7	7
Load Bearing Force [N]	P1–P2	54	94
	P2–P3	53	51
	P3–C	83	55
	C–U	94	103

Post-Fall Recovery Success. The prototype successfully carried the passive mannequin through the full P1→P2→P3→C→U sequence. Because the mannequin provided no voluntary joint torque, the limbs bore the entire system load—a substantially more demanding scenario than the nominal model.

Energy Consumption. Actuator power consumption remained below 32 W per arm throughout recovery, consistent with the modeled trend. During P2→P3 and P3→C, the system operated essentially as a passive cane, driving power to near zero as the astronaut rotated about a single ground contact. The 4-link design consumed 135 J total; the 3-link design consumed only 29 J but at the cost of kinematic feasibility.

Human Body Bracing. A preliminary human participant study found that the prototype ground contact reduced the load borne by the human wearer by up to **55%** at the Kneeling (P3) pose. Table II compares modeled and measured performance metrics.

Higher-than-modeled torques during P1→P2 are expected: the passive mannequin contributed no voluntary torque, so the prototype bore the full load unassisted. Nonetheless, all actuator torques remained below the 400 Nm peak capacity, confirming design feasibility.

V. CONCLUSIONS AND FUTURE WORK

This work presents a complete SuperLimbs design framework grounded in human biomechanics. A "learn-first, design-later" philosophy yields a 4-DoF wearable robotic limb pair that feasibly assists suited astronauts through a full post-fall recovery. The optimal kinematic structure mirrors a human arm, and rearward ground contact placement is the energetically superior bracing strategy. Earth-gravity prototype testing validated the design, with human bracing load reductions up to 55% demonstrated.

Key limitations include: mathematical voluntary torque model uncertainty; sagittal-plane symmetry assumptions ($N = 4$); Earth-gravity and passive-mannequin testing; and off-board power. Future work will target: (i) reduced-gravity testing on lunar-like terrain; (ii) human subject certification at 28 V with on-board batteries; (iii) gripper development for regolith; and (iv) a flight-like modular PLSS attachment for Lunar/Martian EVA. Longer term, the predictable structure of suited recovery trajectories makes this platform well-suited for autonomous control policies, where onboard perception and planning could enable SuperLimbs to detect a fall and trigger recovery without human intervention.

REFERENCES

[1] J. Bridenstine, *Artemis Plan: NASA's Lunar Exploration Program Overview*. NASA, 2020.

[2] J. R. Norcross et al., "Metabolic costs and biomechanics of level ambulation in a planetary suit," NASA, 2010.

[3] B. Holschuh et al., "Characterization of structural, volume and pressure components to space suit joint rigidity," in *39th ICES*, 2009.

[4] S. Sridhar et al., "Space suit and portable life support system center of gravity influence on astronaut kinematics, exertion and efficiency," in *47th ICES*, 2017.

[5] J. Dunn et al., *Evidence Report: Risk of Injury and Compromised Performance due to EVA Operations*. NASA, 2022.

[6] M. L. Gernhardt et al., "Risk of compromised EVA performance and crew health due to inadequate EVA suit systems," in *Human Health and Performance Risks of Space Exploration Missions*, NASA, 2009.

[7] I. P. Abramov et al., "Essential aspects of space suit operating pressure trade-off," *J. Aerospace*, vol. 103, pp. 716–724, 1994.

[8] K. Bethke et al., "Bio-suit development: viable options for mechanical counter pressure," *J. Aerospace*, vol. 113, pp. 426–437, 2004.

[9] F. Parietti and H. Asada, "Supernumerary robotic limbs for human body support," *IEEE Trans. Robot.*, vol. 32, no. 2, pp. 301–311, 2016.

[10] J. Eden et al., "Principles of human movement augmentation and the challenges in making it a reality," *Nature Commun.*, vol. 13, p. 1345, 2022.

[11] E. Ballesteros, M. Brandon, and H. H. Asada, "Supernumerary robotic limbs for next generation space suit technology," in *IEEE ICRA*, 2023, pp. 7519–7525.

[12] E. Ballesteros et al., "Supernumerary robotic limbs to support post-fall recoveries for astronauts," in *IEEE ICRA*, 2024, pp. 2324–2331.

[13] R. D. Crowninshield and R. A. Brand, "A physiologically based criterion of muscle force prediction in locomotion," *J. Biomech.*, vol. 14, no. 11, pp. 793–801, 1981.

[14] A. Diaz and D. Newman, "Musculoskeletal human-spacesuit interaction model," in *IEEE Aerospace Conf.*, 2014.

[15] D. E. Anderson, M. L. Michael, and A. N. Maury, "Maximum voluntary joint torque as a function of joint angle and angular velocity," *J. Biomech.*, vol. 40, no. 14, pp. 3105–3113, 2007.

[16] L. Bordeaux, Y. Hamadi, and L. Zhang, "Propositional satisfiability and constraint programming," *ACM Comput. Surv.*, vol. 38, no. 4, p. 54, 2006.

[17] K. Edelberg et al., "Software system for the Mars 2020 mission sampling and caching testbeds," in *IEEE Aerospace Conf.*, 2018.